TRANSNAV
the International Journal
on Marine Navigation
and Safety of Sea Transportation
http://www.transnav.eu
Volume 17
Number 4
December 2023
DOI: 10.12716/1001.17.04.04

Multi-sensor Integration of Hydroacoustic and Optoelectronic Data Acquired from UAV and USV Vehicles on the Inland Waterbody

O. Specht[1,2]
[1] *Gdynia Maritime University, Gdynia, Poland*
[2] *Marine Technology Ltd., Gdynia, Poland*

ABSTRACT: Hydrographic and photogrammetric measurements in the coastal zone are performed using hydroacoustic and optoelectronic methods, in particular with the use of Unmanned Aerial Vehicles (UAV) and Unmanned Surface Vehicles (USV). It should be remembered that each of the devices registers data in a different spatial reference system. Therefore, before starting the analysis of geospatial data, e.g. terrain relief, it is necessary to carry out the process of their integration (harmonisation). The aim of this article is to present a multi-sensor integration of hydroacoustic and optoelectronic data acquired from UAV and USV vehicles on the inland waterbody. Bathymetric, Light Detection And Ranging (LiDAR) and photogrammetric measurements were carried out on the Lake Kłodno (Poland) in 2022 using the DJI Phantom 4 RTK UAV and two unmanned vessels: AutoDron, which was equipped with a Global Navigation Satellite System (GNSS) Real Time Kinematic (RTK) receiver and a Single Beam Echo Sounder (SBES), as well as HydroDron, on which a GNSS/Inertial Navigation System (INS) and a LiDAR sensor were mounted. The topo-bathymetric chart generated using the Surfer software by the Inverse Distance to a Power (IDP) (p=1) method was developed. A Digital Terrain Model (DTM) generated by the IDP method is characterised by high accuracy. The difference between the interpolated value and the measurement value for the R68 measure is 0.055 m, while for the R95 measure, it has a value of 0.187 m. Research has shown that multi-sensor fusion of geospatial data ensures the possibility of performing bathymetric, LiDAR and photogrammetric measurements in the coastal zone in accordance with the accuracy requirements provided for the International Hydrographic Organization (IHO) Exclusive Order (horizontal position error $\leqslant$ 1 m (p=0.95), vertical position error $\leqslant$ 0.15 m (p=0.95)).

1 INTRODUCTION

The integration of geospatial data recorded with various devices and systems is aimed at transform them to a uniform spatial reference system in order to be able to analyse the measurement results obtained [1–4]. The process of geospatial harmonisation is particularly important in the coastal zone, because it is one of the most dynamic regions on the Earth, due to the fact that it is influenced by the atmosphere, human activities and hydrosphere [5,6]. In addition, the bathymetric monitoring in this zone also helps to prevent negative effects on the aquatic environment and humans [7,8].

Bathymetric and topographic measurements in the coastal zone are carried out using hydroacoustic and optoelectronic devices and systems [7,9]. Hydroacoustic methods use the phenomenon of echolocation, which consists in sending a high-frequency sound wave deep into the water and then receiving the wave reflected from the bottom. The most commonly used hydroacoustic devices and systems are: a hydrometric station, an Inertial

Navigation System (INS), a MultiBeam Echo Sounder (MBES), a positioning system (Differential Positioning System (DGPS) or Real Time Kinematic (RTK)), a Single Beam Echo Sounder (SBES), a SOund Navigation And Ranging (SONAR) and a sound velocity probe [10–15]. The operation of optoelectronic methods consists in converting electrical signals into optical signals and optical signals into electrical signals. The most commonly used optoelectronic devices and systems are: an Airborne Lidar Bathymetry (ALB), an image sensor (a photodiode detector, a photomultiplier tube or Charge-Coupled Device (CCD) and Complementary Met-al-Oxide-Semiconductor (CMOS) cameras), an INS, a laser rangefinder, a positioning system (DGPS or RTK), a RAdio Detection And Ranging (RADAR) and a Terrestrial Laser Scanning (TLS) [16–21].

Liu et al. [22] proposed a Merge-Normalization (MN) method that is suitable for the multi-sensor fusion of bathymetric data in deep ocean waters. This method will help solve the problem of the integration of bathymetric data acquired from different sources in deep waters in order to generate a high-precision Digital Bathymetric Model (DBM). The study used the data acquired using MBES (recorded by the Japan Agency for Marine-Earth Science and Technology (JAMSTEC) and the National Geological and Geophysical Data Center (NGDC) since 2003) and SBES echo sounders (recorded by NGDC since 2000), Electronic Navigational Charts (ENC) (recorded by the National Oceanic and Atmospheric Administration (NOAA) since 2005), as well as Shuttle Radar Topography Mission (SRTM) data sets. The validation study was conducted in the deepest known oceanic trench on the Earth, i.e. the Mariana Trench (Pacific Ocean). The study demonstrated that the multi-sensor fusion of ENC, MBES, SBES and SRTM data enabled the creation of a high-precision digital bathymetric model with a resolution of 100 m. The DBM will enable the exploration of the subduction zone and the seismological mechanism in the Trench region. Moreover, the generated digital bathymetric model was compared with the model generated by the General Bathymetric Chart of the Oceans (GEBCO) in 2014. The results show that the high-resolution DBM obtained by the MN method represents the topographical details of seabed shape better than the GEBCO model.

Lubczonek et al. [23] proposed a method for integrating data acquired using Unmanned Aerial Vehicle (UAV) and Unmanned Surface Vehicle (USV). The aim of the article was to develop a bathymetric chart that includes depths all the way to the shoreline. The study was conducted on the shallow water Lake Dąbie (Poland) with an average depth of 2.61 m. The registered geospatial data was subjected to the process of their integration in order to create a Digital Terrain Model (DTM) of the waterbody. Five methods were applied for terrain modelling: Inverse Distance to a Power (IDP), kriging, Natural Neighbour Interpolation (NNI), radial basis function and triangulation. The study demonstrated that the accuracy of terrain modelling methods used was high (Mean Error (ME) = 0.01 m, Root Mean Square Error (RMSE) = 0.03 m). Therefore, it be concluded that the data acquired using UAV and USV vehicles can be applied for compiling navigational charts of shallow (coastal) waterbodies, analysing the seabed shape in the vicinity of hydrotechnical structures, or archeological mapping.

Masetti et al. [24] proposed Denmark's Depth Model (DDM) in the form of a DBM developed based on hundreds of bathymetric measurements performed within the Danish Exclusive Economic Zone (EEZ). This is the first such DBM with a resolution of 50 m to cover the entire marine area of Denmark. The digital bathymetric model was generated by averaging depth values based on archival data, since it cannot be used for navigation. The DBM contains 75.8% of depth data that were interpolated. 18.1% of depth data were surveyed using a MBES, 5% of depth data were acquired from historical hydrographic soundings and 1.1% of depth data were surveyed using a SBES. The digital bathymetric model covers an area of 232,679 km2 of Danish waters, of which more than 97.5% of data had depths of less than 100 m. The DDM can be downloaded from the Danish Geodata Agency website. The Denmark's Depth Model is also made available via the Open Geospatial Consortium Web Map Service (WMS).

The literature research revealed that the integration of geospatial data acquired by hydroacoustic and optoelectronic methods for topography modelling is commonly applied in the coastal zone. Therefore, the aim of this article is to present a multi-sensor integration of hydroacoustic and optoelectronic data acquired using UAV and USV vehicles on the inland waterbody. Its result will be a three-dimensional DTM of the Lake Kłodno.

This article is structured as follows. Section 2 describes the measurement place (Lake Kłodno) and the course of the performance of hydrographic and photogrammetric measurements using UAV and USV vehicles. Moreover, the section presents the method for elaborating the data recorded during the study. Section 3 presents a three-dimensional DTM in the coastal zone. The paper concludes with final (general and detailed) conclusions that summarise its content.

2 MATERIALS AND METHODS

2.1 *Measurement place*

Lake Kłodno, situated in the Kartuski District (Pomorskie Voivodeship), was selected as the test waterbody. This is an inland waterbody located in the Kaszubski Landscape Park. The total area of the lake is 134.9 ha, the length is 2.0 km and the max depth is 38.5 m. The study conducted by the Chief Inspectorate of Environmental Protection in the years 2017–2018 [25] confirmed that this was a waterbody with a poor water status (second purity class). The transparency of water on this lake was measured using a Secchi disk [26,27]. Research has shown that the transparency of water amounted to 2.4 m [25]. The area under study covered both the land and the water part of the waterbody (Figure 1).

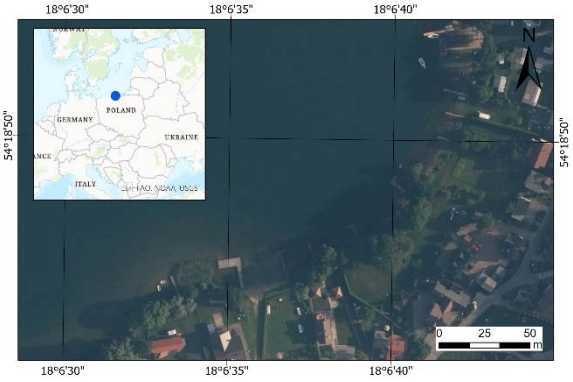

Figure 1. The location of topo-bathymetric measurements conducted on the Lake Kłodno.

2.2 *Realisation of bathymetric, LiDAR and photogrammetric measurements*

The measurement campaign on the Lake Kłodno was conducted on 02-03 June 2022. The study was carried out in four stages. As the first step, bathymetric measurements of the waterbody were performed using the AutoDron USV on which a GNSS RTK receiver and a SBES were mounted [28–30]. The study was conducted along 42 main sounding profiles, which ran perpendicular to the shoreline course direction and were located 10 m apart from each other. They were designed in accordance with the principles for performing hydrographic surveys described in the International Hydrographic Organization (IHO) S-44 standard [31]. Bathymetric measurements were carried out under appropriate hydrometeorological conditions, i.e. in windless weather and at the water level of 0 in the Douglas scale. A total of 7993 points were recorded in the PL-Universal Transverse Mercator (UTM) (zone 34N) and PL-EVRF2007-NH systems. In addition, when performing bathymetric measurements, the water level height was determined based on 21 points surveyed by the geodetic method using a GNSS RTK receiver.

In the second step, the laser scanning of the land area adjacent to the shore was carried out using the HydroDron USV on which a GNSS/INS system and a Light Detection And Ranging (LiDAR) sensor were mounted [32–34]. Hydrographic surveys were conducted on 7 sounding profiles parallel to the shore and located at a distance of 30-100 m from the shoreline. For the recording and georeferencing of the LiDAR point cloud, the HYPACK 2022 software was used. The obtained point cloud was recorded in the PL-UTM system (zone 34N) in the .las format. During the recording, a min. distance threshold value approx. equal to the length of the vehicle was used to reject its own reflections from the HydroDron USV. Moreover, for the georeferencing of the LiDAR point cloud, 141 characteristic points were used (shoreline course and pier corners), determined by the geodetic method using a GNSS RTK receiver.

The third stage of the study involved the surveying of the land and water area of the waterbody by the DJI Phantom 4 RTK UAV. Before starting a flight pass, a photogrammetric control network was designed and used for the georeferencing of images taken by the drone. It comprised 10 wooden markers (30 cm x 30 cm) that were distributed uniformly over the area under study. The geometrical centres of these markers were surveyed using a GNSS RTK receiver. Following this, the performance of photogrammetric measurements started. They needed to be carried out under appropriate meteorological conditions, i.e. no precipitation, windless weather (wind speed not exceeding 6–7 m/s) and a sunny day [35,36]. It was decided to carry out a photogrammetric flight pass at an altitude of 70 m. It was also adopted that the gimbal angle would be 90°, while the longitudinal and transverse coverage of images was set at 80%. During the flight pass, 312 images were recorded.

The final stage of the study involved the determination of waterbody depths in places where it was not possible for the AutoDron USV to access. These included depths between the shoreline and the isobath of 0.6 m. The measurement was carried out by the geodetic method, which involves a surveyor entering water depths to a preset depth using a GNSS receiver mounted on a pole [37–39]. The depth points were located along the same 42 sounding profiles on which the AutoDron USV moved during bathymetric measurements. A total of 218 depth points were recorded in the PL-UTM (zone 34N) and PL-EVRF2007-NH systems [40].

2.3 *Data elaboration*

2.3.1 *Bathymetric data elaboration*

In the first step of the bathymetric data elaboration, the depths recorded erroneously by the SBES were deleted. It should be noted that in the surveyed coastal zone of the Lake Kłodno, there are many areas with ultra-shallow depths (less than 30 cm). In such areas, data is often recorded erroneously as the hydroacoustic signal is repeatedly reflected from the bottom, which necessitates the data cleaning process to be carried out. After cleaning, the point cloud contained 5297 depths. Figure 2 shows the visualisation of the bathymetric data after the data cleaning process. As can be noticed, the removed depths are located close to the shoreline.

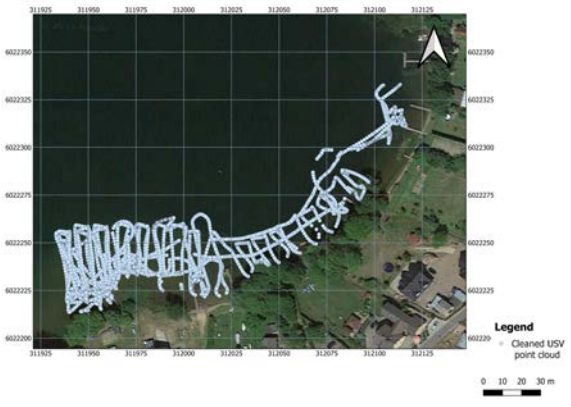

Figure 2. A view of the cleaned USV point cloud.

A draft of the echo sounder transducer (11 cm) was then added to the cleaned depths. Moreover, the depth values were referred to the target vertical datum PL-EVRF2007-NH. These depths were not

referred to the chart datum, as no water level recording was carried out on the Lake Kłodno.

The final stage of work when elaborating the bathymetric data involved the transformation of the plane coordinates recorded in the PL-2000 system into the PL-UTM system. This follows from the data integration assumptions, according to which all the data must be recorded in the PL-UTM system.

Additionally, the depths between the shoreline and the isobath of 0.6 m were attached to the elaborated bathymetric data. In total, 255 recorded points were noted. The data were provided through the bathymetric measurements carried out by the geodetic method and recorded in the PL-2000 plane coordinate system and the PL-EVRF2007-NH normal height system. Therefore, it was necessary to transform the plane coordinates from the PL-2000 system to the PL-UTM system. The transformation was carried out in the QGiS software. Certainly, the geodetic points complemented the bathymetric data recorded by the USV.

2.3.2 *LiDAR data elaboration*

Depending on the geodetic operations being carried out in the area adjacent to the waterbody, optoelectronic devices are used. As regards the measurement campaign in Zawory, the device used was the LiDAR mounted on the HydroDron USV. It was used to record the LiDAR point cloud of the land part along with the shoreline. However, these data were only used to extract the shoreline.

The LiDAR point cloud was georeferenced in the PL-UTM system, as the LiDAR device was integrated with the Ekinox2-U INS on the HydroDron USV. The recording and georeferencing of the LiDAR point cloud were carried out using the HYPACK 2022 software.

The optoelectronic data in the .las format were then uploaded to the CloudCompare and QGIS softwares in order to extract the shoreline. It was decided to extract the shoreline manually, i.e. by drawing it based on the optoelectronic data (Figure 3).

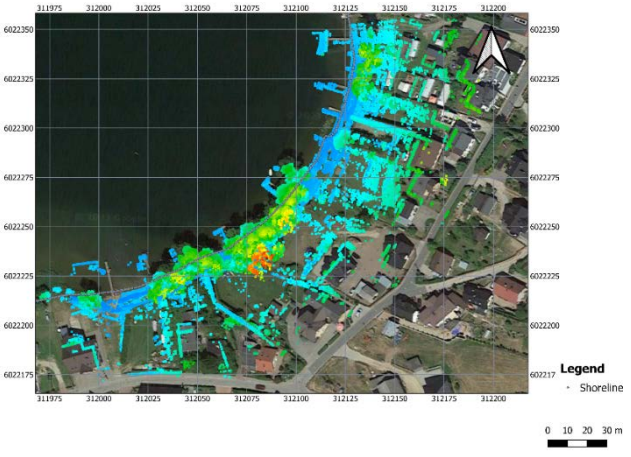

Figure 3. A map showing the LiDAR data along with the shoreline drawn as a point layer.

Initially, the shoreline was drawn as a linear layer. However, for the purposes of data integration, it was exported to the point layer. Moreover, all the points in the layer were given a height value previously surveyed by the GNSS receiver for the 0 m isobath in the PL-EVRF2007-NH system. This value amounted to 160.385 m. The final stage of work involved exporting the points to the .txt format. It was confirmed that the bathymetric data surveyed by the geodetic method could be used to determine the shoreline.

2.3.3 *Photogrammetric data elaboration*

Photogrammetric data elaboration is an important part of the work when developing a DTM in the coastal zone, as these data cover both the land and water part. These are particularly valuable in the event that hydroacoustic devices fail to provide data on shallow areas of up to 0.5 m.

The first stage of work when elaborating the photogrammetric data involved importing the images to the Pix4Dmapper software. Based on the Exchangeable Image File Forma (EXIF) data contained in the photos, the program selected a coordinate system in which the images had been initially recorded. The photos were recorded in the World Geodetic System 1984 (WGS 84). Therefore, it was possible to read the approximate location of the images. The next stage of work was to georeference the photos. Although the images had a coordinate system assigned to them in order to increase their accuracy, it was decided to carry out the previously mentioned georeferencing. In the first step, a .csv file with georeference point coordinates was loaded into the Pix4Dmapper software. Moreover, two pairs of coordinates were entered for a single georeference point. Georeference points were then indicated on the photos (Figure 4).

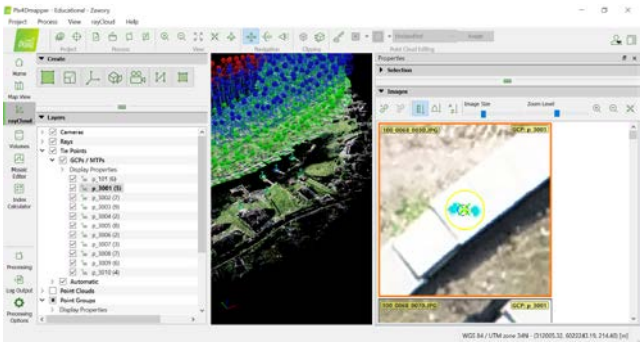

Figure 4. A view of the Pix4Dmapper software panel when matching coordinates to images.

It should be noted that the plane coordinates of georeference points were initially recorded in the PL-2000 system, but were transformed to the PL-UTM system for the DTM. The georeference point heights were recorded in the PL-EVRF2007-NH system. Having selected the relevant images in which the georeference points were visible, the actual georeferencing was started. It is worth mentioning that the Pix4Dmapper software converts coordinates to the target system using the seven parameter transformation. It involves the transformation of coordinates based on previously determined parameters such as the scale factor, rotation matrices and translation vectors. These parameters are calculated through the relationships between the points recorded in the original system (points

recorded on the phots) and the points recorded in the target system (georeference points determined by the GNSS RTK receiver) [41]. In order to assess the accuracy, the differences were compared between the coordinates of georeference points indicated on the images and the coordinates of georeference points surveyed by the GNSS RTK receiver (Table 1).

Table 1. The differences between the coordinates of georeference points indicated on the images and the coordinates of georeference points determined by the GNSS RTK receiver.

No.	Point named	E[1] (m)	dN[2] (m)	dHn[3] (m)
1	p_101 (3D)	–0.006	–0.004	–0.003
2	p_3001 (3D)	–0.008	0.018	0.020
3	p_3002 (3D)	0.001	–0.002	–0.054
4	p_3003 (3D)	0.034	–0.010	0.098
5	p_3004 (3D)	0.051	0.001	–0.158
6	p_3005 (3D)	0.002	–0.036	–0.030
7	p_3006 (3D)	0.041	–0.001	0.142
8	p_3007 (3D)	0.057	0.018	–0.098
9	p_3008 (3D)	0.013	–0.007	–0.001
10	p_3009 (3D)	–0.027	0.005	–0.023
11	p_3010 (3D)	0.016	0.009	0.046
	RMS	0.030	0.014	0.080

The differences between the easting [1], northing [2] and normal height [3] coordinates of georeference points indicated on the images and the coordinates of georeference points determined by the GNSS RTK receiver.

Based on Table 1, it should be stated that the images taken by the UAV have a high degree of accuracy. The Root Mean Square (RMS) of the differences between the coordinates of georeference points indicated on the images and the coordinates of georeference points determined by the GNSS RTK receiver were 0.030 m (easting), 0.014 m (northing) and 0.080 m (normal height).

The next stage of work consisted of the automatic data processing in the software. The UAV point cloud was generated in the form of the GRID Digital Surface Model with a grid spacing of 1 m in the formats of .las, .laz and .xyz.

The final stage of the photogrammetric data elaboration involved point cloud cleaning, which is a mandatory process when developing a DTM. A digital terrain model is created using points located on the land surface, and it does not include land cover features such as, e.g. buildings, trees and vegetation. Therefore, it was necessary to carry out the classification of the point cloud into the features of buildings, infrastructure and vegetation. The automatic classification process was carried out using the Pix4Dmapping software. The above-mentioned features were then deleted. Moreover, the water part of the area was removed for elaboration purposes. The cleaned UAV point cloud contained 14 227 points (Figure 5).

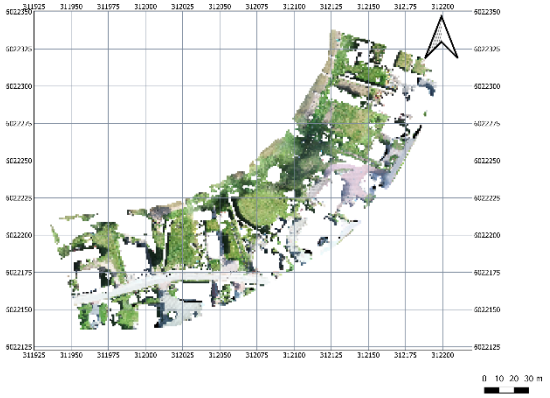

Figure 5. A view of the cleaned UAV point cloud.

3 RESULTS

Based on the data recorded during the measurement campaign in Zawory, a DTM was developed in the Surfer software. The digital terrain model was created using the IDP method [42]. The total number of points used for the interpolation of the waterbody along with the adjacent strip of land by the IDP method was 19 996. The IDP method was chosen because, for the model of the waterbody adjacent to the beach along with the strip of land in Gdynia, one of the highest coefficients of determination (0.998) was obtained for this method. Additionally, what is characteristic of the IDP method is that the influence of measurement points on the values of interpolated points, which are more distant from the node, decreases with an increase in the power exponent. This is of particular importance when developing a topo-bathymetric model based on a large dataset.

The IDP method is as follows [42]:

$$z_{IDP}(x,y)=\frac{\sum_{i}^{n} w_i(x,y)\times z_i}{\sum_{i}^{n} w_i(x,y)} \quad (1)$$

where:
$z_{IDP}(x,y)$ – height value of the interpolated (unknown) point by the IDP method (m);
x, y – easting and northing of the interpolated (unknown) point (m);
n –number of interpolating (known) points (–);
i – numbering representing successive interpolating (known) points (–);
$w_i(x,y)$ – weight value of the i-th point in the IDP method (–);
z_i – height of the i-th measurement point (m).

The weight values are dependent on the smoothing parameter [43]:

$$w_i(x,y)=\frac{1}{\left[d_i(x,y)+\delta\right]^p} \quad (2)$$

where:

$d_i(x,y)$ –distance between the interpolated (unknown) point and the i-th point (m);
δ – smoothing parameter (m);
p – exponent (–).

In the model, the exponent p=1 was applied. Moreover, a range of the data interpolating a particular point was defined for the IDP (p=1) method. It was established that the min. number of interpolating points would be 16. The topo-bathymetric chart generated using the Surfer software by the IDP (p=1) method is presented on Figure 6.

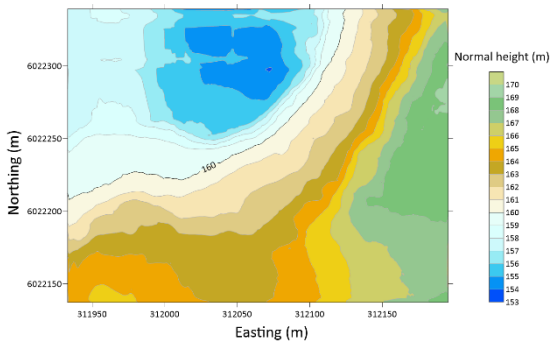

a)

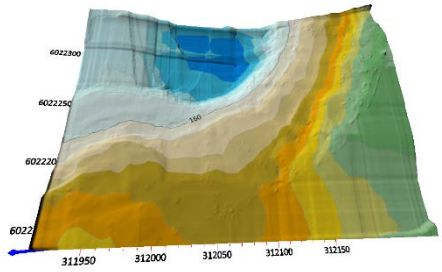

b)

Figure 6. A topo-bathymetric chart of the waterbody adjacent to the beach along with the strip of land in Zawory, developed based on bathymetric, LiDAR and photogrammetric measurements using the IDP (p=1) method (a) and its 3D visualisation (b).

In the generated GRID model, the min. depth value was 153.909 m, while the max height value was 169.835 m. The accuracy of the interpolated DTM (Figure 6) in relation to the measurements was determined using the RMSE to be 0.089 m and the Mean Absolute Error (MAE) to be 0.055 m. The coefficient of determination was obtained at a level of 0.999, which means that the fit of the model to the measurement data is very good. The difference between the interpolated value and the measurement value for the R68 measure is 0.055 m, while for the R95 measure, it has a value of 0.187 m.

4 CONCLUSIONS

Multi-sensor integration of hydroacoustic and optoelectronic data is a multi-stage task that should be considered on a case-by-case basis, depending on the input data. The article presents the methodology for performing bathymetric, LiDAR and photogrammetric measurements in the Lake Kłodno coastal zone. Moreover, it describes all the stages of bathymetric, LiDAR and photogrammetric data elaboration. The conducted work resulted in the development of a DTM.

A very important stage in the creation of DTM is data elaboration. At the beginning, work was started on the UAV point cloud. Initially, UAV data covered the Lake Kłodno area along with the adjacent land. However, in order to develop a digital terrain model, only data on the surface are needed, which means that the data recorded on buildings, trees and other built features are redundant. Therefore, these data need to be removed, which is possible through the classification of objects. When creating the DTM, the automatic classification of objects in the Pix4Dmapper software was used. This was followed by work on the bathymetric data. Here, the crucial stage was to clean the data manually and refer them to the shoreline height. In turn, the shoreline was drawn manually based on the LiDAR data. As can be noticed, all the described data elaboration stages included manual data edition processes. This means that multi-sensor data integration cannot be performed completely automatically.

Based on the measurements performed, it can be concluded that only complex surveys provide sufficient data to create an accurate DTM. A digital terrain model generated by the IDP method is characterised by high accuracy. The difference between the interpolated value and the measurement value for the R68 measure is 0.055 m, while for the R95 measure, it has a value of 0.187 m. Research has shown that multi-sensor fusion of geospatial data ensures the possibility of performing bathymetric, LiDAR and photogrammetric measurements in the coastal zone in accordance with the accuracy requirements provided for the IHO Exclusive Order (horizontal position error $\leqslant$ 1 m (p=0.95), vertical position error $\leqslant$ 0.15 m (p=0.95)).

FUNDING

This research was funded by the National Centre for Research and Development in Poland, grant number LIDER/10/0030/L-11/19/NCBR/2020. Moreover, this research was funded from the statutory activities of Gdynia Maritime University, grant number WN/PI/2023/03.

REFERENCES

1. Abdalla, R. Introduction to Geospatial Information and Communication Technology (GeoICT); Springer: Berlin/Heidelberg, Germany, 2016; pp. 105–124.
2. Brivio, P.A.; Colombo, R.; Maggi, M.; Tomasoni, R. Integration of Remote Sensing Data and GIS for Accurate Mapping of Flooded Areas. Int. J. Remote Sens. 2002, 23, 429–441.
3. Brown, D.G.; Riolo, R.; Robinson, D.T.; North, M.; Rand, W. Spatial Process and Data Models: Toward Integration of Agent-based Models and GIS. J. Geogr. Syst. 2005, 7, 25–47.
4. Popielarczyk, D.; Templin, T. Application of Integrated GNSS/Hydroacoustic Measurements and GIS Geodatabase Models for Bottom Analysis of Lake

Hancza: The Deepest Inland Reservoir in Poland. Pure Appl. Geophys. 2014, 171, 997–1011.
5. Cao, W.; Wong, M.H. Current Status of Coastal Zone Issues and Management in China: A Review. Environ. Int. 2007, 33, 985–992.
6. Cicin-Sain, B.; Knecht, R.W. Integrated Coastal and Ocean Management: Concepts and Practices, 1st ed.; Island Press: Washington, DC, USA, 1998.
7. Specht, M.; Specht, C.; Mindykowski, J.; Dąbrowski, P.; Maśnicki, R.; Makar, A. Geospatial Modeling of the Tombolo Phenomenon in Sopot Using Integrated Geodetic and Hydrographic Measurement Methods. Remote Sens. 2020, 12, 737.
8. Specht, M.; Stateczny, A.; Specht, C.; Widźgowski, S.; Lewicka, O.; Wiśniewska, M. Concept of an Innovative Autonomous Unmanned System for Bathymetric Monitoring of Shallow Waterbodies (INNOBAT System). Energies 2021, 14, 5370.
9. Lewicka, O.; Specht, M.; Stateczny, A.; Specht, C.; Brčić, D.; Jugović, A.; Widźgowski, S.; Wiśniewska, M. Analysis of GNSS, Hydroacoustic and Optoelectronic Data Integration Methods Used in Hydrography. Sensors 2021, 21, 7831.
10. Kang, M. Overview of the Applications of Hydroacoustic Methods in South Korea and Fish Abundance Estimation Methods. Fish. Aquat. Sci. 2014, 17, 369–376.
11. Makar, A. Determination of USV's Direction Using Satellite and Fluxgate Compasses and GNSS-RTK. Sensors 2022, 22, 7895.
12. Makar, A. Method of Determination of Acoustic Wave Reflection Points in Geodesic Bathymetric Surveys. Annu. Navig. 2008, 14, 1–89.
13. Parente, C.; Vallario, A. Interpolation of Single Beam Echo Sounder Data for 3D Bathymetric Model. Int. J. Adv. Comput. Sci. Appl. 2019, 10, 6–13.
14. Specht, C.; Specht, M.; Dabrowski, P. Comparative Analysis of Active Geodetic Networks in Poland. In Proceedings of the 17th International Multidisciplinary Scientific GeoConference (SGEM 2017), Albena, Bulgaria, 27 June–6 July 2017.
15. Wlodarczyk-Sielicka, M.; Stateczny, A. Comparison of Selected Reduction Methods of Bathymetric Data Obtained by Multibeam Echosounder. In Proceedings of the 2016 Baltic Geodetic Congress (BGC 2016), Gdańsk, Poland, 2–4 June 2016.
16. Kondo, H.; Ura, T. Navigation of an AUV for Investigation of Underwater Structures. Control Eng. Pract. 2004, 12, 1551–1559.
17. Noureldin, A.; Karamat, T.B.; Georgy, J. Inertial Navigation System. In Fundamentals of Inertial Navigation, Satellite-based Positioning and Their Integration; Springer: Berlin/Heidelberg, Germany, 2013; pp. 125–166.
18. Specht, M. Method of Evaluating the Positioning System Capability for Complying with the Minimum Accuracy Requirements for the International Hydrographic Organization Orders. Sensors 2019, 19, 3860.
19. Stateczny, A. Radar Water Level Sensors for Full Implementation of the River Information Services of Border and Lower Section of the Oder in Poland. In Proceedings of the 17th International Radar Symposium (IRS 2016), Kraków, Poland, 10–12 May 2016.
20. Wehr, A.; Lohr, U. Airborne Laser Scanning—An Introduction and Overview. ISPRS J. Photogramm. Remote Sens. 1999, 54, 68–82.
21. Williams, R.; Brasington, J.; Vericat, D.; Hicks, M.; Labrosse, F.; Neal, M. Chapter Twenty–Monitoring Braided River Change Using Terrestrial Laser Scanning and Optical Bathymetric Mapping. In Developments in Earth Surface Processes; Elsevier: Amsterdam, Netherlands, 2011; Volume 15, pp. 507–532.
22. Liu, Y.; Wu, Z.; Zhao, D.; Zhou, J.; Shang, J.; Wang, M.; Zhu, C.; Luo, X. Construction of High-resolution Bathymetric Dataset for the Mariana Trench. IEEE Access 2019, 7, 142441–142450.
23. Lubczonek, J.; Kazimierski, W.; Zaniewicz, G.; Lacka, M. Methodology for Combining Data Acquired by Unmanned Surface and Aerial Vehicles to Create Digital Bathymetric Models in Shallow and Ultra-shallow Waters. Remote Sens. 2022, 14, 105.
24. Masetti, G.; Andersen, O.; Andreasen, N.R.; Christiansen, P.S.; Cole, M.A.; Harris, J.P.; Langdahl, K.; Schwenger, L.M.; Sonne, I.B. Denmark's Depth Model: Compilation of Bathymetric Data within the Danish Waters. Geomatics 2022, 2, 486-498.
25. Chief Inspectorate of Environmental Protection. Assessment of the State of Lake Waterbodies in 2017-2018 - table. Available online: http://www.gios.gov.pl/pl/mkoopz/8-pms/99-jeziora (accessed on 3 February 2023). (In Polish)
26. Kabiri, K. Accuracy Assessment of Near-shore Bathymetry Information Retrieved from Landsat-8 Imagery. Earth Sci. Inform. 2017, 10, 235–245.
27. Menberu, Z.; Mogesse, B.; Reddythota, D. Evaluation of Water Quality and Eutrophication Status of Hawassa Lake Based on Different Water Quality Indices. Appl. Water Sci. 2021, 11, 61.
28. Specht, C.; Specht, M.; Cywiński, P.; Skóra, M.; Marchel, Ł.; Szychowski, P. A New Method for Determining the Territorial Sea Baseline Using an Unmanned, Hydrographic Surface Vessel. J. Coast. Res. 2019, 35, 925–936.
29. Specht, M.; Specht, C.; Lasota, H.; Cywiński, P. Assessment of the Steering Precision of a Hydrographic Unmanned Surface Vessel (USV) along Sounding Profiles Using a Low-cost Multi-Global Navigation Satellite System (GNSS) Receiver Supported Autopilot. Sensors 2019, 19, 3939.
30. Specht, M.; Specht, C.; Szafran, M.; Makar, A.; Dąbrowski, P.; Lasota, H.; Cywiński, P. The Use of USV to Develop Navigational and Bathymetric Charts of Yacht Ports on the Example of National Sailing Centre in Gdańsk. Remote Sens. 2020, 12, 2585.
31. IHO. IHO Standards for Hydrographic Surveys, 6th ed.; Special Publication No. 44; IHO: Monaco, Monaco, 2020.
32. Stateczny, A.; Błaszczak-Bąk, W.; Sobieraj-Żłobińska, A.; Motyl, W.; Wisniewska, M. Methodology for Processing of 3D Multibeam Sonar Big Data for Comparative Navigation. Remote Sens. 2019, 11, 2245.
33. Stateczny, A.; Burdziakowski, P.; Najdecka, K.; Domagalska-Stateczna, B. Accuracy of Trajectory Tracking Based on Nonlinear Guidance Logic for Hydrographic Unmanned Surface Vessels. Sensors 2020, 20, 832.
34. Stateczny, A.; Kazimierski, W.; Gronska-Sledz, D.; Motyl, W. The Empirical Application of Automotive 3D Radar Sensor for Target Detection for an Autonomous Surface Vehicle's Navigation. Remote Sens. 2019, 11, 1156.
35. Kacprzak, M.; Wodziński K. Execution of Photo Mission by Manned Aircraft and Unmanned Aerial Vehicle. Transactions of the Institute of Aviation 2016, 2, 130–141. (In Polish)
36. Witek, M.; Jeziorska, J.; Niedzielski, T. Possibilities of Using Unmanned Air Photogrammetry to Identify Anthropogenic Transformations in River Channel. Landform Analysis 2013, 24, 115–126. (In Polish)
37. Czaplewski, K.; Specht, C. Determination of Coast and Base Line by GPS Techniques. Navigation and Hydrography 2002, 14, 137–144.
38. Harley, M.D.; Turner, I.L.; Short, A.D.; Ranasinghe, R. Assessment and Integration of Conventional, RTK-GPS and Image-derived Beach Survey Methods for Daily to Decadal Coastal Monitoring. Coast. Eng. 2011, 58, 194–205.
39. Specht, C.; Weintrit, A.; Specht, M.; Dąbrowski, P. Determination of the Territorial Sea Baseline—

Measurement Aspect. IOP Conf. Ser. Earth Environ. Sci. 2017, 95, 1–10.
40. Council of Ministers of the Republic of Poland. Ordinance of the Council of Ministers of 15 October 2012 on the National Spatial Reference System; Council of Ministers of the Republic of Poland: Warsaw, Poland, 2012. (In Polish)
41. Lewicka, O.; Specht, M.; Stateczny, A.; Specht, C.; Dyrcz, C.; Dąbrowski, P.; Szostak, B.; Halicki, A.; Stateczny, M.; Widźgowski, S. Analysis of Transformation Methods of Hydroacoustic and Optoelectronic Data Based on the Tombolo Measurement Campaign in Sopot. Remote Sens. 2022, 14, 3525.
42. Ohlert, P.L.; Bach, M.; Breuer, L. Accuracy Assessment of Inverse Distance Weighting Interpolation of Groundwater Nitrate Concentrations in Bavaria (Germany). Environ. Sci. Pollut. Res. 2022, 30, 9445–9455.
43. Tomczak, M., Spatial Interpolation and its Uncertainty Using Automated Anisotropic Inverse Distance Weighting (IDW) - Cross-Validation/Jackknife Approach. Journal of Geographic Information and Decision Analysis 1998, 2, 18–30.